FERMILAB-PUB-05-330-AD

Beam Profile Diagnostics for the Fermilab Medium Energy Electron Cooler

A. Warner, G. Kazakevich, S. Nagaitsev, G. Tassotto, W. Gai, R. Konecny

***Abstract*—The Fermilab Recycler ring will employ an electron cooler to store and cool 8.9 GeV antiprotons. The cooler will be based on a Pelletron electrostatic accelerator working in an energy-recovery regime. Several techniques for determining the characteristics of the beam dynamics are being investigated. Beam profiles have been measured as a function of the beam line optics at the energy of 3.5 MeV in the current range of 10^{-4}-1 A, with a pulse duration of 2 μs. The profiles were measured using optical transition radiation produced at the interface of a 250 μm aluminum foil and also from YAG crystal luminescence. In addition, beam profiles measured using multi-wire detectors were investigated. These three diagnostics will be used together to determine the profile dynamics of the beam. In this paper we report the results so far obtained using these techniques.**

I. Introduction

In this paper we report on development and test of the electron beam diagnostics that was done at a bench of the prototype facility designed for electron cooling of the anti-proton beam. The facility was based on a 5 MV Pelletron accelerator operating in an energy recovery regime [1]. Investigations of the beam diagnostics were performed in a pulse mode. The accelerated 3.5 MeV electron beam had a pulse duration of 2 μs with a 1 Hz repetition rate, the accelerated current was variable in the range of 10^{-4}-1 A [2].

The beam diagnostics using transition radiation techniques, as well as the YAG-crystal as a luminescent detector and the multi-wire secondary emission monitor were utilized to obtain the parameters of the electron beam at the bench and to study the beam dynamics at the facility. The beam initial conditions, spatial uniformity and size will be measured and monitored with the systems developed at this test bench.

Experimental Set-Up

The system of the beam diagnostics consisting of a multi-wire monitor, a YAG crystal and a transition radiation monitor was assembled at the test bench located in the straight part the supply beam line of the electron cooling facility, Fig. 1.

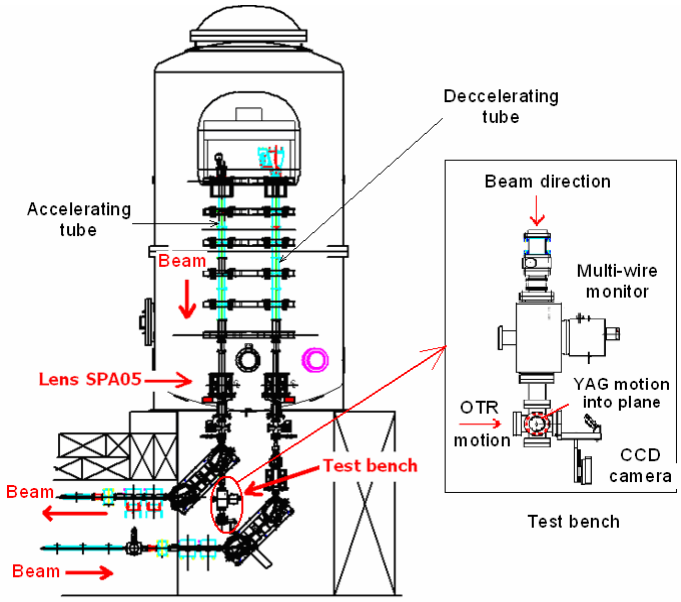

Fig. 1 Location of the test bench at the electron cooling facility

The multi-wire monitor was mounted inside cylindrical vacuum chamber (upper part of the test bench) downstream the first bending magnet of the facility. The monitor was made from two planes (X and Y) of 48 tungsten mutually perpendicular wires. The two planes were separated by 10 mm. The wires in both planes were 25 μm in diameter and were spaced 0.5 mm apart. The signal from each wire was read independently, processed and displayed.

The YAG crystal used for a fluorescent beam profile monitoring was a 50 mm square single crystal with a thickness of 0.1 mm mounted on the moving stage in the six-way

This work was supported in part by the U.S. Department of Energy

A. Warner is with Fermi National Accelerator Lab, P O Box 500, Batavia, IL 60510 USA (telephone: 630-840-6119, email: warner@fnal.gov).

G. Kazakevich is with Fermi National Accelerator Lab, P O Box 500, Batavia, IL 60510 USA (telephone: 630-840-5028, email: kazakevi@fnal.gov).

S. Nagaitsev is with Fermi National Accelerator Lab, P O Box 500, Batavia, IL 60510 USA (telephone: 630-840-4397, email:nsergei@fnal.gov).

G. Tassotto is with Fermi National Accelerator Lab, P O Box 500, Batavia, IL 60510 USA (telephone: 630-840-4325, email:tassotto@fnal.gov).

W. Gai is with Argonne National Laboratory, 9700 S. Cass Avenue, Argonne, IL USA (telephone: 630-252-6560, wg@hep.anl.gov).

R. Konecny is with Argonne National Lab, 9700 S. Cass Avenue, Argonne IL USA (telephone: 630-252-6597, email:rsk@hep.anl.gov).

vacuum chamber (lower part of the test bench) located downstream the multiwires monitor. The crystal surface had an angle of 45 degrees to the incident beam.

Two types of transition radiation (TR) screens mounted on the other moving stage and positioned obliquely to the incident electron beam were tested in the set-up; initial measurements were done with a thin screen made from a 5 μm nitrocellulose substrate having mirror coating with 1200 Å of aluminum; this produces an ultra-flat pellicle surface with up to 1/10λ reflection on central areas. Subsequent measurements were done with a 250 μm roughly polished aluminum foil having a noticeably lower reflectance than that of the first screen.

The axes of motion of the YAG crystal and the transition radiation screen (x, y) were orthogonal to each other in the six-way chamber. As a result the devices could only be inserted into the beam when one or the other was removed. However the multi-wire monitor could be inserted independently during a measurement. Simplified layout of the test bench monitors is presented in Fig. 2.

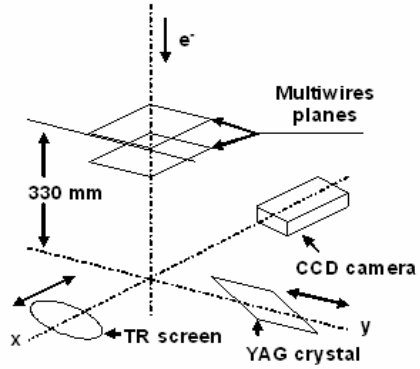

Fig. 2 Layout of the test bench monitors. Arrows show the directions of motion of the TR-screen and YAG crystal.

The transition radiation in the optical range as well as the luminescence from the YAG-crystal was detected with a CCD camera located at the distance of ≈ 50 cm from the light sources and shielded with 5 cm lead bricks to suppress the Bremsstrahlung. The focal length and the relative aperture of the objective were 50 mm and 1.4 respectively.

The beam sizes, position and profiles were measured as a function of the Pelletron gun current, which was varied by changing of the pulse voltage of the gun control electrode. These parameters were also measured as a function of the current of the focusing lens SPA05 which was mounted upstream of the beam, before the entrance to the test bench, Fig. 1. Results obtained using the optical monitors were compared with data obtained with the multi-wire detector.

Transition Radiation and YAG Image Processing

Images taken from the optical monitors were digitized and saved in an uncompressed format using application software that was developed using LabView and IMAQ vision utility tools. This type of development differs from the standard application in that it incorporates image digitization, image display, as well as image analysis and system calibration in a real-time module. The image analysis tools were used to combine techniques that compute statistics and measurements based on the gray-level intensities of the image pixels; a linear (convolution) filters were then applied to remove unwanted background. The profile data were extracted from images to establish color scale data and produce the beam profile or 3-D representation of the data. Calibration to real-scale coordinates was done by using a set of 125 μm tungsten wires that were placed over the transition radiation screen to form a rectangular 10 mm x 10 mm grid. Beam profiles data were measured to study the beam optics parameters and also for optimization of the current density range. The improved spatial resolution afforded by these monitors and real-time techniques allows for measurement of the beam initial conditions at the test-bench prior to transporting the beam through the entire cooling system.

Transition Radiation Monitors

Predicted more than 50 years ago, transition radiation [3] is now widely used in many laboratories as a powerful method for diagnostics of beams of charged particles. The radiation is generated when a charged particle beam crosses the interface between two media of different dielectric constants; for beam profile diagnostics it is usually the radiation emitted from a vacuum-metal boundary. In practice a metal foil is inserted into the beam line at an oblique angle to the beam direction of motion. As a result transition radiation is emitted in both the forward and backward directions. The method typically utilizes the optical part of the transition spectrum, so-called Optical Transition Radiation (OTR).

The OTR monitors have several excellent and unique features for beam diagnostics; they produce a wide emission spectrum including visible light with well defined directionality and polarization. In addition the simplicity of detectors has lead to widespread use of the method. The surface nature of OTR also allows the use of very thin screens which reduces beam scattering and Bremsstrahlung radiation.

OTR detectors will be used in the Fermilab electron cooling facility to measure the real-time profile dynamics of the beam.

The intensity of the backward OTR photons in the frequency range of $d\omega$ at oblique incidence to the surface of an ideal metal screen with relativistic electrons can be expressed as [4], [5]:

$$\frac{d^2W}{d\Omega\, d\omega} = J(\theta,\omega) \approx \frac{e^2\beta^2}{\pi^2 c}\cdot\frac{\sin^2\theta}{(1-\beta^2\cos^2\theta)^2},$$

where e is the electron charge, c is the velocity of light, β is the velocity of the electrons in units of c and θ is the angle between the wave vector of the radiation and the mirror-reflected electron velocity vector in the point of the incidence. The shape of the spectral density versus θ is shown in Fig. 3. The intensity of the OTR is maximal at the angle of: $\theta \approx 1/\beta\gamma$.

Note that for particle beams in the mid to low energy range the angular distribution of the OTR is not sharply peaked. As a result, the low value of the optical acceptance causes loss of

light. Our optics provided an observation angle $\alpha \approx 0.04$ rad. In this case the coefficient of collection of the OTR photons, n_c, (relative number of detected photons) determined by integration of the function $J(\theta,\omega)$ over the angle has the respective value: $n_c \approx 10^{-3}$.

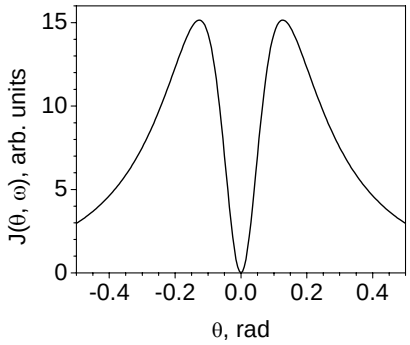

Fig. 3 Spectral density of OTR versus θ by the energy of electrons of 3.5 MeV

Simple estimations show that for a beam spot size area of 100 x 100 pixels, and a beam current of 1 A with the pulse duration of 2 μs, the number of photons should be of $\sim 10^4$ photons/pixel per pulse. In this case the threshold current for detected profiles for the above conditions can be expected to be ≈ 0.1 A. To decrease the minimal detected current and increase the sensitivity of the OTR diagnostics one could use a cooled CCD camera or an intensified CCD camera.

A restored 3-D image of the electron beam with the current of 0.975 A and lens SPA05 current of 14 A using the LabView based techniques is presented in Fig. 4. The image was taken with the roughly polished OTR screen.

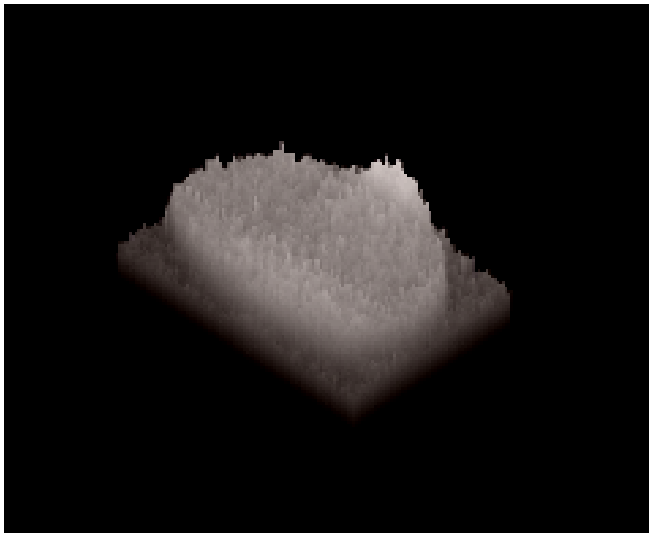

Fig. 4. 3-D image of the electron beam obtained with OTR monitor.

OTR diagnostics was used to study the dependence of the beam profile on the lens SPA05 focusing and also on the voltage of the gun control electrode. Fig. 5 shows measured X-profiles as a function of the lens current for the beam current ≈1A. In all of the profiles clearly one can see marks from the scale. The space resolution of the OTR diagnostics is better than 0.1 mm with the CCD camera and optics that was used.

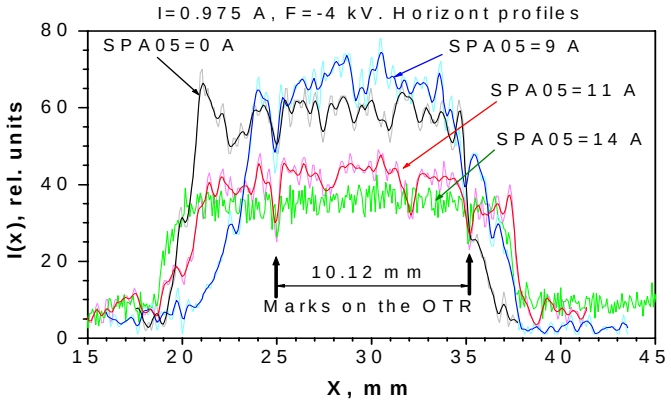

Fig. 5 Variation of the beam X-profile versus SPA05 lens current.

The dependence of the beam profile on the beam current obtained by varying the pulse voltage of the gun control electrode is presented in Fig. 6. The average value of the measured current density was in the range of 3-4 mA/mm^2.

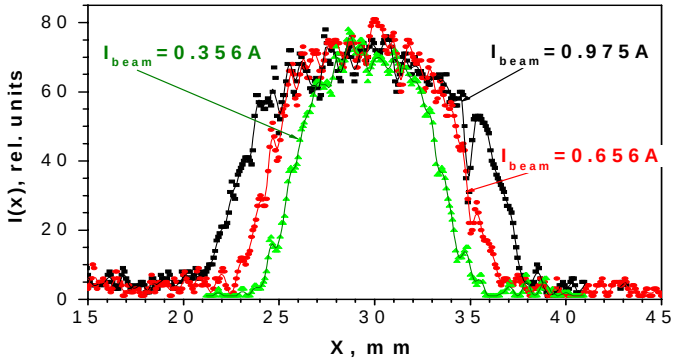

Fig. 6 Dependence of the beam X-profile on the Pelletron beam current

Note that OTR monitors images have no saturation or limitation in dynamic range and yield of the photons is proportional to intensity of the monitored beam.

YAG Scintillation Monitor

YAG (Yttrium Aluminum Garnet) single crystal scintillators are now frequently used for charged particle beams and X-ray detection as well as for electron and X-ray imaging screens due to the high resistance to radiation damage. The photon yield for the YAG crystals is $\approx 8 \cdot 10^3$ *photons/MeV,* so for the crystal which has a thickness of 0.1 mm, the yield should be of $\approx 0.73 \cdot 10^3$ photons per passing electron. The light emitted from the crystal was collected under the same optical conditions as that of measurements made with the OTR monitor and the coefficient of collection of the photons had the value of $n_c \approx 3 \cdot 10^{-3}$. In this case the threshold current for the image of the beam spot with size of 100 x 100 pixels, and

pulse duration of 2 μs can be estimated to be of ≈ 1 μA in the pulse mode.

This high sensitivity of the scintillator is convenient for the investigations of low-current beams. Higher beam currents (above 1 mA) resulted in the saturation of the YAG crystal, Fig. 7. To avoid saturation in CCD camera during the measurements, we used neutral density optical attenuators.

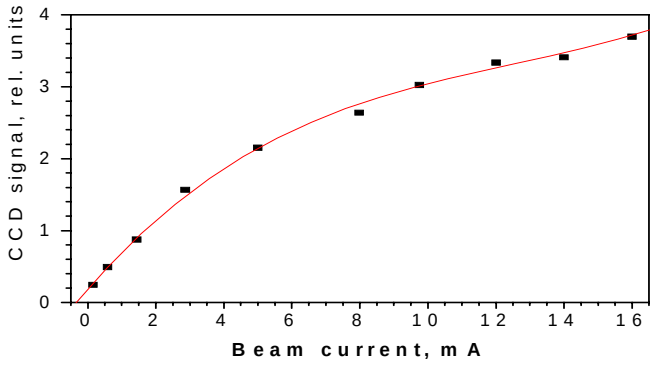

Fig. 7. Dependence of YAG-monitor signal on the beam current.

The low current beam image taken with the YAG crystal is shown in Fig. 8. The current in lens SPA05 was 9 A for this data. The average current density on the crystal corresponded to 0.013 mA/mm^2. The respective restored beam profile measured along the X axis is shown in Fig. 9.

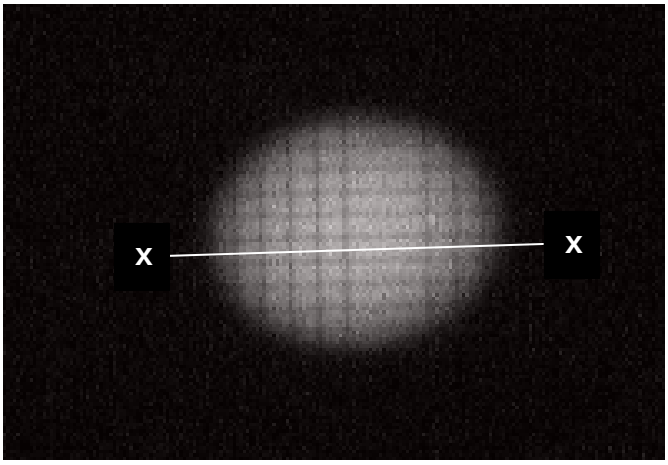

Fig. 8. The image of the low-current beam from YAG monitor.

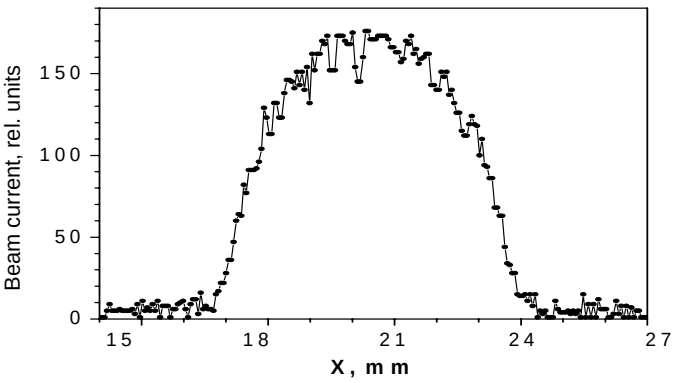

Fig. 9. Restored X-profile of low-current beam measured with the YAG monitor.

In both these figures one can see shadow of the multi-wire monitor located at 330 mm upstream to the position of the YAG-monitor. The shadow is visible because of scattering of the electron beam on the wires of the monitor. The spatial resolution of the measurements made with the YAG and the OTR monitors is approximately equal. The 3-D shape of the beam distribution restored using techniques based on LabView is presented in Fig. 10. Note that the profile is for a very low current and the measured beam size is therefore much smaller.

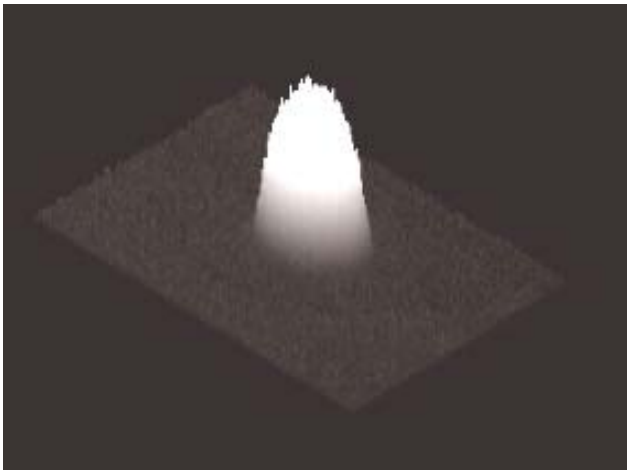

Fig. 10. 3-D image of the electron beam obtained with YAG monitor

Multi-wire Beam Monitor.

Data from the multi-wire X-Y monitor were used for measurements of the beam sizes and to study the beam optics with the test bench. The correlation between the spatial distribution of the beam density and the charge distribution as measured by the multi-wire monitor in a given plane is expressed by an integral equation having no singular solution in common case. However, in case of an axial-symmetric beam the integral equation has the form:

$$\lambda(x) = 2\int_{x}^{R} n(r) \cdot \frac{rdr}{\sqrt{r^2 - x^2}},$$

where: x is coordinate of the wire, $\lambda(x)$ is the measured charge distribution in the plane of multi-wire monitor, $n(r)$ is beam density distribution. In our case of weak dependence of the beam density on the radius, $n(r) \approx constant$ and the equation can be transformed to the following:

$$n(m) \approx \frac{n_{\max}}{\sqrt{n_{\max}^2 - (m - n_{\max})^2}} \cdot \lambda(m),$$

where $m=0,1...2n_{max}$; m- number of wires charged by the passing beam, n_{max}. is the number of wires respective to the beam radius.

Fig. 11 shows the beam X-profiles restored from the charge distribution data of the multi-wire monitor with the beam pulse current of 0.975 A and the lens SPA05 current of 0.0 A.

The profiles were restored for different fits corresponding to various diameter of the electron beam passing through 30 or 32 wires respectively. The dotted line shows the profile measured with the OTR-monitor located at 330 mm downstream relatively the multi-wire monitor. Smoothing of the dotted OTR-image is shown by solid line.

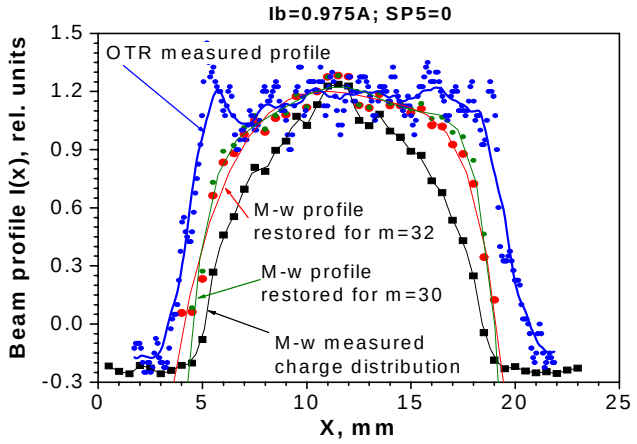

Fig. 11. Restored beam X-profile obtained with the multiwires monitor data. For comparison are also plotted the distribution of the charge of the multiwires monitor in the X-plane and the X-profile of the electron beam measured by downstream OTR-monitor.

The difference in the size of the beam X-profile measured with the OTR and the multi-wire monitors has a value of ≈ 2 mm, which is primarily due to the divergence of the beam at the location of the multi-wires (≈ 3-4 mrad). Note, that the spatial resolution of the multi-wire monitor depends on the gap between wires; in our case it is ≈ 0.5 mm.

The OTR measured profile is a direct measurement of the beam distribution and size and is independent of any type of symmetry of the beam. The OTR profile resolution depends on the efficiency of the collection of the light, the pixel resolution and the noise level associated with the CCD image.

Conclusion

Beam diagnostics based on optical transition radiation monitors, YAG scintillator and multi-wire monitors has been developed and tested for use in the Fermilab Recycler electron cooling system. The OTR diagnostics provides real-time profiles with improved spatial resolution better than 100 μm in the pulse current range of 0.1-1.0 A with the pulse duration of 2 μs. Several OTRs will be employed in the cooling system to measure the size and density distribution of the beam. The YAG monitor diagnostic provides approximately the same resolution for the pulse currents less than 1 mA and will be used to verify low current transport of beam to the cooler. The multi-wire secondary emission monitors provide space resolution approximately of 0.5 mm for the beam size measurements with the pulse current of ≥ 0.1 A. The monitor will be used in the return line section of the cooler.

Acknowledgements

We wish to thank Arnold Germain Jr. and Daniel Schoo for their technical contributions.

References

[1] S. Nagaitsev, G. Saewert, A. Shemyakin, A. Warner, "Diagnostics for the 5 MeV electron cooling system," Nucl. Instr. and Meth. In Phys. Res. A441 (2000), pp. 246-254.

[2] A. Shemyakin, A. Burov, K. Carlson, V. Dudnikov, B. Kramper, T. Kroc, J. Leibfritz, M. McGee, S. Nagaitsev, G. Saewert, C. Schmidt, A. Warner, S. Seletsky, V. Tupikov, "Attainment of an MeV-range, DC electron beam for the Fermilab cooler," Nucl. Instr. and Meth. in Phys. Res. A 532 (2004) pp. 403-407

[3] V.L. Ginzburg and I.M. Frank, "Radiation from a Uniformly Moving Electron passing from One Medium to Another", Journ. of Experimental and Theoretical Physics (JETP) V.16 15, (1946)

[4] L.D. Landau, and E.M. Lifshitz, Electrodynamics of Continuous Media (Addison-Wesley, Reading, MA 1960).

[5] L. Wartski, S. Roland, J. Lasalle, M. Bolore, and G. Filippi, "Interference phenomenon in optical transition radiation and its application to particle beam diagnostics and multiple-scattering measurements", Journ. of Applied Physics, V. 46, No. 8,1975.